PHYSICAL REVIEW B **80**, 041405(R) (2009)

Electron spin relaxation in graphene: The role of the substrate

Christian Ertler,* Sergej Konschuh, Martin Gmitra, and Jaroslav Fabian
Institute for Theoretical Physics, University of Regensburg, 93040 Regensburg, Germany
(Received 6 May 2009; revised manuscript received 19 June 2009; published 24 July 2009)

Theory of the electron-spin relaxation in graphene on the SiO_2 substrate is developed. Charged impurities and polar-optical surface phonons in the substrate induce an effective random Bychkov-Rashba-like spin-orbit coupling field, which leads to spin relaxation by the D'yakonov-Perel' mechanism. Analytical estimates and Monte Carlo simulations show that the corresponding spin relaxation times are between micro- to milliseconds, being only weakly temperature dependent. It is also argued that the presence of adatoms on graphene can lead to spin lifetimes shorter than nanoseconds.

DOI: 10.1103/PhysRevB.80.041405 PACS number(s): 72.25.Rb, 73.61.Wp, 73.50.Bk

Since the experimental realization of graphene, a single stable two-dimensional monolayer of carbon atoms arranged in a honeycomb lattice, considerable research has been done to enlighten its peculiar electronic transport properties originating from the Dirac-like band structure at the K and K' points in the momentum space.[1] Long spin relaxation times and phase coherence lengths in graphene are expected based on the weak atomic spin-orbit (SO) coupling in carbon ($Z=6$). However, recent spin injection measurements based on a nonlocal spin valve geometry[2–4] revealed surprisingly short spin relaxation times of only about 100–200 ps, being only weakly dependent on the charge density and temperature. These results appear puzzling, although the low mobilities of the samples (about 2000 cm^2/Vs) suggest that the measured spin relaxation times are likely due to extrinsic effects.[2]

Very recent experiments on the charge transport in graphene affirmed the importance of the underlying substrate.[5–7] At low temperatures the transport properties have been shown to be dominated by scattering from the charged impurities residing in the substrate.[6,8] The conductivity of graphene placed on a SiO_2 substrate starts to decrease above 200 K. The observed temperature and density dependence of the resistivity are most likely explained by remote phonon scattering due to occurrence of polar-optical surface modes in the substrate.[9–11]

These findings naturally raise the question if (i) charged impurities and (ii) remote surface phonons are also relevant for the spin relaxation in graphene. As argued here both mechanisms provide a temperature-dependent, random spin-orbit coupling field, which limits the spin relaxation via the D'yakonov-Perel' (DP) mechanism.[12–14] The calculated spin relaxation times are micro- to milliseconds. In addition, we give estimates for the spin relaxation times due to the possible presence of adatoms on graphene. For reasonable adatom densities the spin lifetimes can be lower than nanoseconds.

Several other mechanisms have already been investigated theoretically, such as the spin relaxation due to the corrugations (ripples) of graphene and due to exchange interaction with local magnetic moments,[15] or spin-orbit coupling mediated relaxation based on boundary scattering, heavy impurities, and effective gauge fields due to topological disorder.[16]

Near the K and K' points the carrier dynamics can be described by an effective low-energy Hamiltonian[17] of the form $H_0=\hbar v_f(\tau_z\sigma_x k_x+\sigma_y k_y)$. Here, $v_f=10^6$ m/s denotes the Fermi velocity, $\mathbf{k}$ is the wave vector with respect to $K(K')$, and τ and σ are the Pauli matrices with $\tau_z=\pm 1$ describing the states at the K and K' points, respectively, and $\sigma_z=\pm 1$ describing the states on the A and B sublattice of the honeycomb lattice. The inclusion of the microscopic SO interaction results in an additional term in the effective low-energy Hamiltonian, $H_I=-\lambda_I+\lambda_I\tau_z\sigma_z s_z$ as shown either by group theoretical arguments[18] or by second-order perturbation theory of a microscopic tight-binding model.[19–21] Here, the real spin is represented by the s_z Pauli matrix and λ_I denotes the intrinsic SO constant (SOC). The intrinsic SOC opens a gap $\Delta_I=2\lambda_I$ at the Dirac point, making graphene theoretically a spin Hall insulator.[18] Recent first-principles calculations give $\Delta_I=0.024$ meV,[22] large enough to influence electronics of intrinsic or weakly charged graphene only somewhat below 1 K.

If an electric field is applied perpendicular to the graphene plane, the inversion symmetry is lifted and group theory allows for an additional Bychkov-Rashba (BR) term of the form $H_{\mathrm{BR}}=\lambda_{\mathrm{BR}}(\tau_z\sigma_x s_y-\sigma_y s_x)$.[18,19,21,23] From first-principles calculations[22] a linear relationship between the BR constant and the electric field, $\lambda_{\mathrm{BR}}(\mathbf{r})=\zeta_{\mathrm{BR}}E_z(\mathbf{r})$, is found, with $\zeta_{\mathrm{BR}}=0.005$ meV/(V/nm). The proper knowledge of λ_{BR} is of great importance for our quantitative results below since in the DP mechanism the spin relaxation rate depends quadratically on λ_{BR}.

The resulting effective 8×8 Hamiltonian $H_{\mathrm{eff}}=H_0+H_I+H_{\mathrm{BR}}$ is easily diagonalized, yielding the same eigenvalues at the K and K' points,

$$\varepsilon_{m\nu}=\nu(\lambda_{\mathrm{BR}}-\nu\lambda_I)+m\sqrt{\varepsilon^2+(\lambda_{\mathrm{BR}}-\nu\lambda_I)^2}, \qquad (1)$$

with $\varepsilon=\hbar v_f|k|$, $\nu=\pm 1$, and the band index $m=1$ for electrons (e) and $m=-1$ for holes (h), respectively. We define spin vectors $\mathbf{n}^\tau_{m\nu}=\mathbf{s}^\tau_{m\nu}/|\mathbf{s}^\tau_{m\nu}|$ as normalized expectation values of the spin operator $\mathbf{s}^\tau_{m\nu}=\langle\psi|\hat{\mathbf{S}}|\psi\rangle$ with respect to the eigenstates $|\psi\rangle=|\tau,\mathbf{k},m,\nu\rangle$ ($\tau=K,K'$) of the total Hamiltonian H_{eff}. The vectors are in-plane and result in $\mathbf{n}^\tau_{e+}=\mathbf{n}^\tau_{h-}=(-\sin\varphi,\cos\varphi,0)$ and $\mathbf{n}^\tau_{e-}=\mathbf{n}^\tau_{h+}=(\sin\varphi,-\cos\varphi,0)$ with φ denoting the polar angle of the wave vector $\mathbf{k}$. In the case of $\varepsilon\gg\lambda_R+\lambda_I$, i.e., if the Fermi energy is much greater than ≈ 0.03 meV (a condition usually fulfilled in gated or doped graphene) the electron and hole motion can be decoupled. By successive unitary rotation of H_{eff} first into the

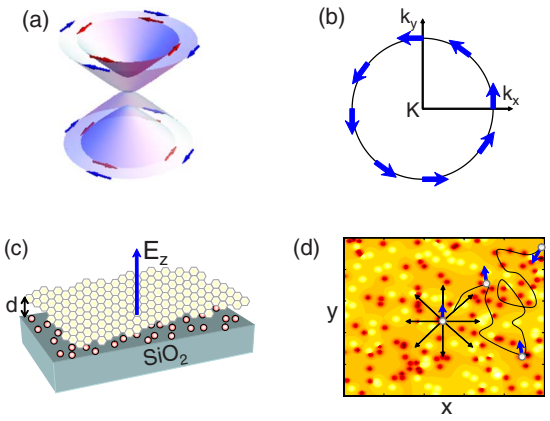

FIG. 1. (Color online) (a) The Dirac cones when spin-orbit coupling is included. The arrows indicate the spin vectors $\mathbf{n}_{m\nu}^{K}$ as defined in the text. (b) Effective magnetic field directions (Bychkov-Rashba field) along the Fermi circle of electrons at the K point (the field is the same at the K' point). (c) Graphene layer on the top of a SiO_2 substrate with charged impurities, which induce an electric-field component E_z perpendicular to the plane breaking the inversion symmetry of graphene. (d) Illustration of the spin relaxation in a spatially random potential due to the charged carriers. In the Monte Carlo simulations the spin dynamics is sampled over random trajectories with different initial momenta.

eigenbasis of H_0 and then into the spin basis with respect to the direction $\mathbf{n}=(-\sin\varphi,\cos\varphi,0)$ an effective BR-type 2×2 Hamiltonian can be obtained for both holes and electrons,

$$\tilde{H}_{\text{eff}} = m(\varepsilon - \lambda_I) + m\lambda_{\text{BR}}\mathbf{n}(\mathbf{k})\cdot\mathbf{s} \tag{2}$$

with $\mathbf{s}$ denoting the Pauli-spin matrices. $\tilde{H}_{\text{eff}}$ is the same for K and K', as guaranteed by time-reversal symmetry.

Comparison with the original BR Hamiltonian in semiconductor heterostructures of the form $H_{\mathbf{k}}=\hbar\boldsymbol{\Omega}(\mathbf{k})\cdot\mathbf{s}/2$ shows that SOC coupling in graphene effectively acts on the electrons spin as an in-plane magnetic field of *constant* amplitude but $\mathbf{k}$-dependent direction, as illustrated in Figs. 1(a) and 1(b). In this effective field the spin precesses with a frequency of $\Omega=2\lambda_{\text{BR}}/\hbar$. As shown by D'yakonov and Perel'[12,13] random scattering induces motional narrowing of this spin precession causing spin relaxation. The spin relaxation rates for the DP mechanism for the αth spin component generally result in $1/\tau_{s,\alpha}=\tau^*(\langle\boldsymbol{\Omega}_{\mathbf{k}}^2\rangle-\langle\boldsymbol{\Omega}_{\alpha}^2\rangle)$, with τ^* denoting the correlation time of the random spin-orbit field and $\langle\ldots\rangle$ indicates averaging over the Fermi surface. Due to the polar angle dependence, in graphene the correlation time exactly coincides with the momentum relaxation time $\tau^*=\tau_p$.[13,14] Hence, for graphene the spin relaxation time results in $1/\tau_{s,z}=\tau_p(2\lambda_{\text{BR}}/\hbar)^2$ and $\tau_{s,\{x,y\}}=2\tau_{s,z}$.

First, we investigate spin relaxation due to charged impurities residing in the substrate as schematically illustrated in Fig. 1(c). Impurity scattering is a dominant scattering mechanism governing the transport properties of graphene.[5,6,8] Due to the fluctuations of the impurity concentration a random unscreened electric field perpendicular to the graphene plane and hence a spatially random BR field $\lambda_{\text{BR}}(\mathbf{r})=\zeta_{\text{BR}}E_z(\mathbf{r})$ arise. As shown by Sherman[24] in the case of semiconductor quantum wells, the randomness of the BR field in the real space already causes spin relaxation even without any scattering in the $\mathbf{k}$-space. The correlation length of the random BR field is on the scale of the distance d of the impurity layer from the graphene sheet.[24] Therefore, the spin relaxation time for a ballistically moving electron can be estimated as follows: if the electron passes through a domain of the lateral size of the correlation length of the BR field, the spin precesses by $\delta\varphi=\Omega_{\text{BR}}d/v_f$. At some time t the electron has passed through $t/(d/v_f)$ different domains, and in the picture of a random walk it follows that $\langle\Delta\varphi\rangle=\delta\varphi\sqrt{t/(d/v_f)}$. The spin is relaxed if $\langle(\Delta\varphi)^2\rangle\approx1$ yielding the condition $1/\tau_s\approx4/\hbar^2\langle\lambda_{\text{BR}}^2\rangle d/v_f$. Hence, in a semiclassical picture for the orbital motion $\mathbf{r}(t)$ of the electron, the spin experiences a random BR field *both* in the real space (Sherman mechanism) and in the reciprocal space due to momentum scattering (DP mechanism).

We numerically calculate the spin relaxation time by performing Monte Carlo (MC) simulations for the spin dynamics. For this purpose we use a random but quenched impurity distribution of a given density and sample over the random particles trajectories starting with different initial momenta, as illustrated in Fig. 1(d). The trajectories are generated according to the scattering probability of the screened impurity potentials in the graphene sheet calculated in the random-phase approximation following Ref. 6.

Along any given semiclassical trajectory $[\mathbf{r}(t),\mathbf{k}(t)]$ the spin dynamics can be described by the Bloch equation

$$\frac{d\mathbf{s}}{dt} = \Omega_{\text{BR}}[\mathbf{r}(t)](\mathbf{n}[\mathbf{k}(t)]\times\mathbf{s}). \tag{3}$$

The spin relaxation time is then calculated by averaging over the asymptotics of all trajectories since for times much greater than the mean-free time $t\gg\tau_{\text{mfp}}$ the spin components relax as $s_\alpha(t)=s_\alpha(0)\exp(-t/\tau_{s,\alpha})$.[24]

Figure 2 shows the calculated spin relaxation time as a function of the Fermi energy E_f for a dirty SiO_2 substrate, $n_{\text{imp}}=4\times10^{12}$ cm^{-2} and for a cleaner sample, $n_{\text{imp}}=4\times10^{11}$ cm^{-2}, taking into account only impurity scattering. For all simulations we use the *ab initio* BR parameter $\zeta_{\text{BR}}=0.005$ meV/(V/nm) and an effective impurity distance of $d=0.4$ nm from the graphene layer.[6,9] The symbols refer to the MC-simulation results and the solid lines indicate analytic fits of the form $1/\tau_s=\tau_{\text{imp}}(E_f)\Omega_{\text{eff}}^2$, with τ_{imp} denoting the momentum relaxation time due to impurities. Since the cross section of the screened long-ranged Coulomb potential is proportional to the Fermi wavelength $\lambda_f\sim k_f^{-1}$,[10] the momentum relaxation time increases with increasing Fermi energy yielding a decreasing spin relaxation time, as illustrated in Fig. 2

The second important spin relaxation mechanism induced by the SiO_2 substrate is due to polar-optical surface phonons. In the case of SiO_2 there are two dominant surface phonons with energies of $\hbar\omega_s^{(1)}=59$ meV and $\hbar\omega_s^{(2)}=155$ meV, respectively, which provide a temperature dependent electric-field variance given by[25]

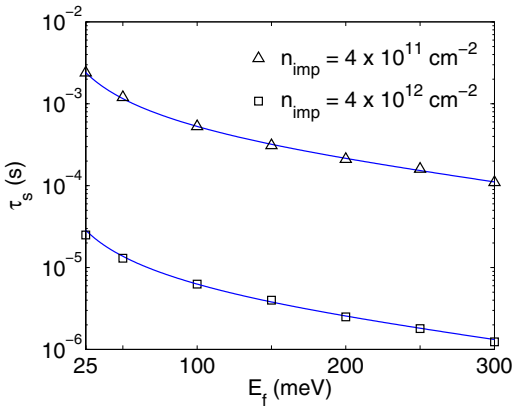

FIG. 2. (Color online) Calculated spin relaxation time τ_s as a function of the Fermi energy E_f, taking into account only impurity scattering, for two different impurity densities in the substrate at $T=0$ K. The symbols indicate MC-simulation results, and the solid lines are analytic fits of the form $1/\tau_s=\tau_{\mathrm{imp}}(E_f)\Omega_{\mathrm{eff}}^2$ with $\Omega_{\mathrm{eff}}=3.3\times10^9$ s^{-1} (for squares) and $\Omega_{\mathrm{eff}}=1.1\times10^8$ s^{-1} (for triangles).

$$\langle E_{z,i}^2\rangle(T)=\beta_i\frac{\hbar\omega_s^{(i)}}{4\pi\varepsilon_0}\frac{(1+2n_s^{(i)})}{4d^3}, \tag{4}$$

with ε_0 denoting the dielectric constant and $n_s^{(i)}$ standing for the Bose-Einstein occupation factors of the phonon mode i. The individual strengths of these remote phonon-scattering modes are given by the parameters $\beta_1=0.025$ and $\beta_2=0.062$, which fulfill the relation $\beta=\Sigma_i\beta_i=(\varepsilon_s-\varepsilon_\infty)/(\varepsilon_s+1)(\varepsilon_\infty+1)$, with β giving a measure of the total polarizibility of the dielectric interface[9] and ε_s and ε_∞ denoting the static and high-frequency dielectric constant, respectively. Due to the randomness of the electrons' motion the spin experiences an effective electric field and, hence, a random BR field. The effective spectral correlation function of the phonon field $\langle E_z(t)E_z(t')\rangle$ will include an exponential decay with the momentum relaxation time τ_m yielding a Lorentzian renormalization factor $E_{\mathrm{eff},i}^2=\langle E_{z,i}^2\rangle/[1+(\omega_s^{(i)}\tau_m)^2]$.[14] If $\omega_s\tau_m\gg1$ (as for graphene on SiO_2), the effective electric field can be found by qualitative arguments: for long-wave phonons the spin precesses by $\delta\varphi=\Omega_{\mathrm{BR}}\tau_{\mathrm{ph}}$ in the characteristic time $\tau_{\mathrm{ph}}=1/\omega_s$. The momentum scattering leads to a random walk with typical step times of τ_m. The spin is relaxed if the variance $\langle\delta\varphi\rangle^2=(t/\tau_m)\delta\varphi$ reaches one, yielding for the spin relaxation time $1/\tau_s=\Omega_{\mathrm{BR}}^2\tau_m/(\omega_{\mathrm{ph}}\tau_m)^2=\Omega_{\mathrm{eff}}^2\tau_m$ giving an effective field of $E_{\mathrm{eff}}^2=E^2/(\omega_{\mathrm{ph}}\tau_m)^2$.

For the MC simulations we took into account momentum scattering due to charged impurities in SiO_2, optical surface phonons,[9] and acoustic phonons of the graphene sheet.[11] The resulting total momentum relaxation rate $1/\tau_{\mathrm{tot}}=1/\tau_{\mathrm{imp}}+1/\tau_{\mathrm{sph}}(T)+1/\tau_{\mathrm{ac}}(T)$ is illustrated in Fig. 3, showing that the impurity scattering remains dominant up to room temperature but with an exponentially increasing contribution coming from the surface phonons and a linearly growing contribution due to acoustic phonon scattering. The random BR field is calculated from the electric field originating from the impurities and the polar surface phonons.

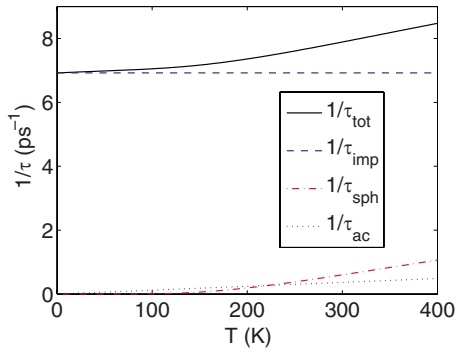

FIG. 3. (Color online) Calculated inverse momentum relaxation times $1/\tau$ as function of temperature T for impurity (imp) scattering (with $n_{\mathrm{imp}}=4\times10^{11}$ cm^{-2}), surface phonon (sph), and acoustic phonon (ac) scattering at $E_f=100$ meV.

The temperature dependence of the spin relaxation time for a fixed Fermi energy of $E_f=100$ meV for different impurity densities is shown in Fig. 4, where the solid lines indicate again fits of the form $1/\tau_s=\tau_{\mathrm{tot}}(T)[2\zeta_{\mathrm{BR}}E_{\mathrm{eff}}/\hbar]^2$. The MC simulations reveal that the spin relaxation time is almost temperature independent. This is caused by the nearly perfect counterbalancing of the increasing electric field and the decreasing momentum relaxation time with temperature. As for the relaxation of the momentum, impurities dominate the spin relaxation compared to the mechanism of optical surface phonons, which causes a decrease in τ_s by about 10–20 %.

Can we relate our results to the experimental findings of τ_s of 100–200 ps?[2] Even considering the uncertainties in d or in the charge density in the substrate, such small values for τ_s can be hardly explained by the substrate effects. Indeed, the measured samples have short mean-free times of about $\tau_{\mathrm{mfp}}\approx50$ fs,[2] which suggest a high impurity density of about $n_{\mathrm{imp}}=2-4\times10^{12}$ cm^{-2}.[6] However, the times $\tau_s\approx100$ ps would require SO constants orders of magnitude higher than the ones obtained by first-principles calculations[22] used here. In the experimental samples graphene was additionally

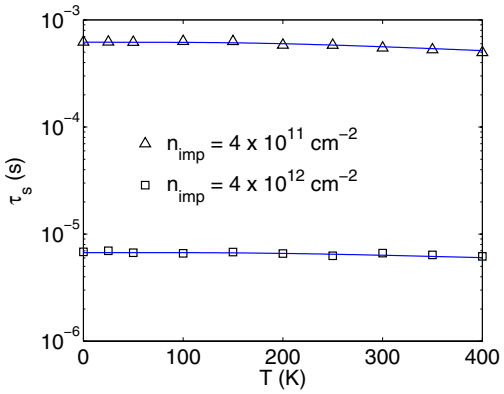

FIG. 4. (Color online) Calculated spin relaxation time τ_s versus temperature T taking into account impurity, surface phonon, and acoustic phonon scattering at $E_f=100$ meV. The symbols refer to MC data, and the solid lines are fits of the form $1/\tau_s=\tau_{\mathrm{tot}}(T)[2\zeta_{\mathrm{BR}}E_{\mathrm{eff}}/\hbar]^2$ with $E_{\mathrm{eff}}=0.21$ V/nm (for squares) and $E_{\mathrm{eff}}=0.007$ V/nm (for triangles).

coated by an Al_2O_3 layer to realize working tunnel barrier contacts. This likely brings metallic adatoms, which induce a stronger spin-orbit coupling strength, as has been reported for a full layer of Au atoms in contact with graphene in which several orders of magnitude larger BR constant of about 13 meV were found;[26] similar large SO constants were predicted for impurities on graphene.[27] Suppose an adatom induces a local spin-orbit splitting of magnitude ≈ 10 meV. The splitting spreads a distance s of perhaps a few bond lengths. Let the average distance between the randomly positioned adatoms be r. Then the DP spin relaxation rate is $1/\tau_s \approx \Omega^2 \tau (s/r)^2$. The rate is reduced from that for a homogeneous splitting by $(s/r)^2$, which renormalizes Ω^2 due to the finite effective adatoms area. As a generic example we take s to be two bond lengths, $s \approx 3$ Å, and a reasonable distance $r \approx 10$ nm, we get the spin relaxation time $\tau_s \approx 50$ ps (using $\tau \approx 100$ fs), being of the same order of magnitude as the measured value.[2] The adatom mechanism depends strongly on the adatom type and density, making it experimentally testable.

In summary, we showed that charged impurities and polar-optical surface phonons of the substrate generate a random Bychkov-Rashba SO-field, which leads to an almost temperature-independent spin relaxation in graphene. The calculated spin relaxation times give the upper bounds of what one can expect experimentally for a clean graphene on a substrate. The above calculation also shows that spin injection and spin transport should be severely limited if metallic electrodes are deposited directly on graphene.

This work has been supported by the DFG (Grants No. SFB 689 and No. SPP 1285). We thank E. Sherman for very valuable and inspiring discussions.

*christian.ertler@physik.uni-regensburg.de

[1] A. K. Geim and K. S. Novoselov, Nature Mater. **6**, 183 (2007).
[2] N. Tombros, C. Jozsa, M. Popinciuc, H. T. Jonkman, and B. J. van Wees, Nature (London) **448**, 571 (2007).
[3] N. Tombros, S. Tanabe, A. Veligura, C. Jozsa, M. Popinciuc, H. T. Jonkman, and B. J. van Wees, Phys. Rev. Lett. **101**, 046601 (2008).
[4] C. Józsa, M. Popinciuc, N. Tombros, H. T. Jonkman, and B. J. van Wees, Phys. Rev. Lett. **100**, 236603 (2008).
[5] J.-H. Chen, C. Jang, S. Adam, M. S. Fuhrer, E. D. Williams, and M. Ishigami, Nat. Phys. **4**, 377 (2008).
[6] S. Adam and S. Das Sarma, Solid State Commun. **146**, 356 (2008).
[7] J. Sabio, C. Seoánez, S. Fratini, F. Guinea, A. H. Castro Neto, and F. Sols, Phys. Rev. B **77**, 195409 (2008).
[8] S. Adam, E. H. Hwang, V. M. Galitski, and S. Das Sarma, Proc. Natl. Acad. Sci. U.S.A. **104**, 18392 (2007).
[9] S. Fratini and F. Guinea, Phys. Rev. B **77**, 195415 (2008).
[10] F. Guinea, J. Low Temp. Phys. **153**, 359 (2008).
[11] J. Chen, C. Jang, S. Xiao, M. Ishigami, and M. S. Fuhrer, Nat. Nanotechnol. **3**, 206 (2008).
[12] M. I. D'yakonov and V. I. Perel', Fiz. Tverd. Tela (Leningrad) **13**, 3581 (1971) [Sov. Phys. Solid State **13**, 3023 (1971)].
[13] M. I. D'yakonov and V. I. Perel', in *Optical Orientation, Modern Problems in Condensed Matter Science*, edited by F. Meier and B. P. Zakharchenya (North-Holland, Amsterdam, 1984), Vol. 8, p. 40.
[14] J. Fabian, A. Matos-Abiague, C. Ertler, P. Stano, and I. Žutić, Acta Phys. Slov. **57**, 565 (2007).
[15] D. Huertas-Hernando, F. Guinea, and A. Brataas, Eur. Phys. J. Spec. Top. **148**, 177 (2007).
[16] D. Huertas-Hernando, F. Guinea, and A. Brataas, arXiv:0812.1921 (unpublished).
[17] D. P. DiVincenzo and E. J. Mele, Phys. Rev. B **29**, 1685 (1984).
[18] C. L. Kane and E. J. Mele, Phys. Rev. Lett. **95**, 226801 (2005).
[19] H. Min, J. E. Hill, N. A. Sinitsyn, B. R. Sahu, L. Kleinman, and A. H. MacDonald, Phys. Rev. B **74**, 165310 (2006).
[20] Y. Yao, F. Ye, X.-L. Qi, S.-C. Zhang, and Z. Fang, Phys. Rev. B **75**, 041401(R) (2007).
[21] D. Huertas-Hernando, F. Guinea, and A. Brataas, Phys. Rev. B **74**, 155426 (2006).
[22] M. Gmitra, S. Konschuh, C. Ertler, C. Ambrosch-Draxl, and J. Fabian, arXiv:0904.3315 (unpublished).
[23] E. I. Rashba, Phys. Rev. B **79**, 161409(R) (2009).
[24] E. Y. Sherman, Appl. Phys. Lett. **82**, 209 (2003).
[25] S. Q. Wang and G. D. Mahan, Phys. Rev. B **6**, 4517 (1972).
[26] A. Varykhalov, J. Sánchez-Barriga, A. M. Shikin, C. Biswas, E. Vescovo, A. Rybkin, D. Marchenko, and O. Rader, Phys. Rev. Lett. **101**, 157601 (2008).
[27] A. Castro Neto and F. Guinea, arXiv:0902.3244 (unpublished).